Electronic Supplementary Material (ESI) for Inorganic Chemistry Frontiers.

Supporting Information

Open-framework aluminum hexacyanoferrate as cathode materials for high voltage aqueous zinc-ion batteries: Effect of Al^{3+} cation on three-phase transition of $AlFe(CN)_6$

Yulin Kong [a], *Yawei Xiao* [a], *Liang Chen* [b], *Shuotao Zhang* [b], *Zhaoping Liu* [b*], *Yude Wang* [a,c*]

[a] *National Center for International Research on Photoelectric and Energy Materials, School of Materials and Energy, Yunnan University, Kunming 6500504, China.*

[b] *Ningbo Institute of Materials Technology and Engineering, Chinese Academy of Sciences (CAS), Ningbo 315201, China*

[c] *Yunnan Key Laboratory of Carbon Neutrality and Green Low-carbon Technologies, Yunnan University, Kunming 6500504, China.*

*E-mail addresses: liuzp@nimte.ac.cn (Z. P. Liu), ydwang@ynu.edu.cn (Y. D. Wang)

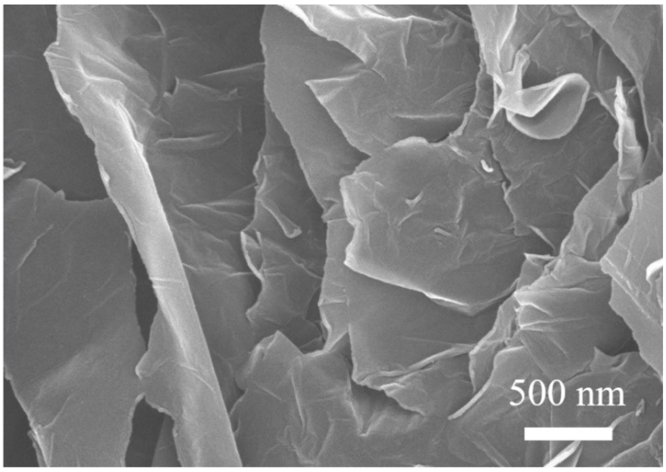

Fig. S1 Graphene sheet obtained through thermal exfoliation of graphene oxide.

Fig. S2 The digital photo of AlHCF (blue) and AlHCF/Gr (black).

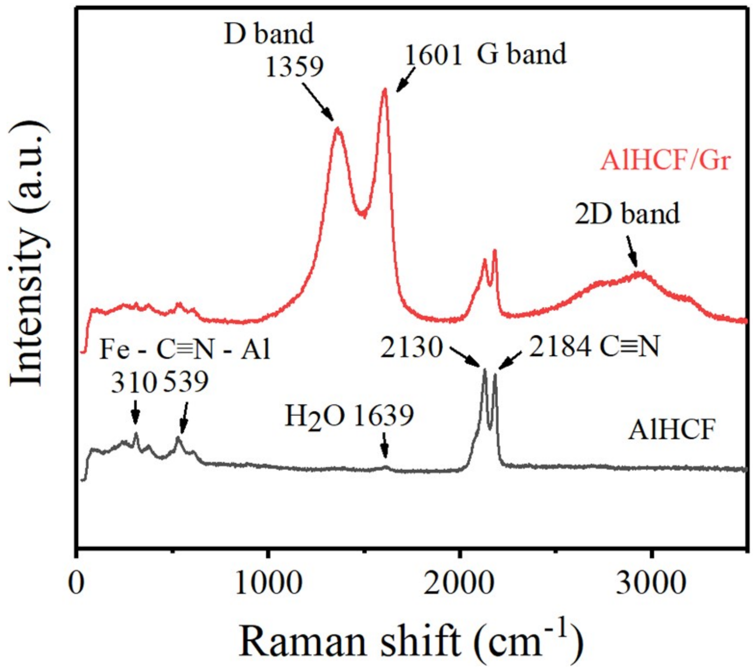

Fig. S3 Raman spectra of AlHCF and AlHCF/Gr.

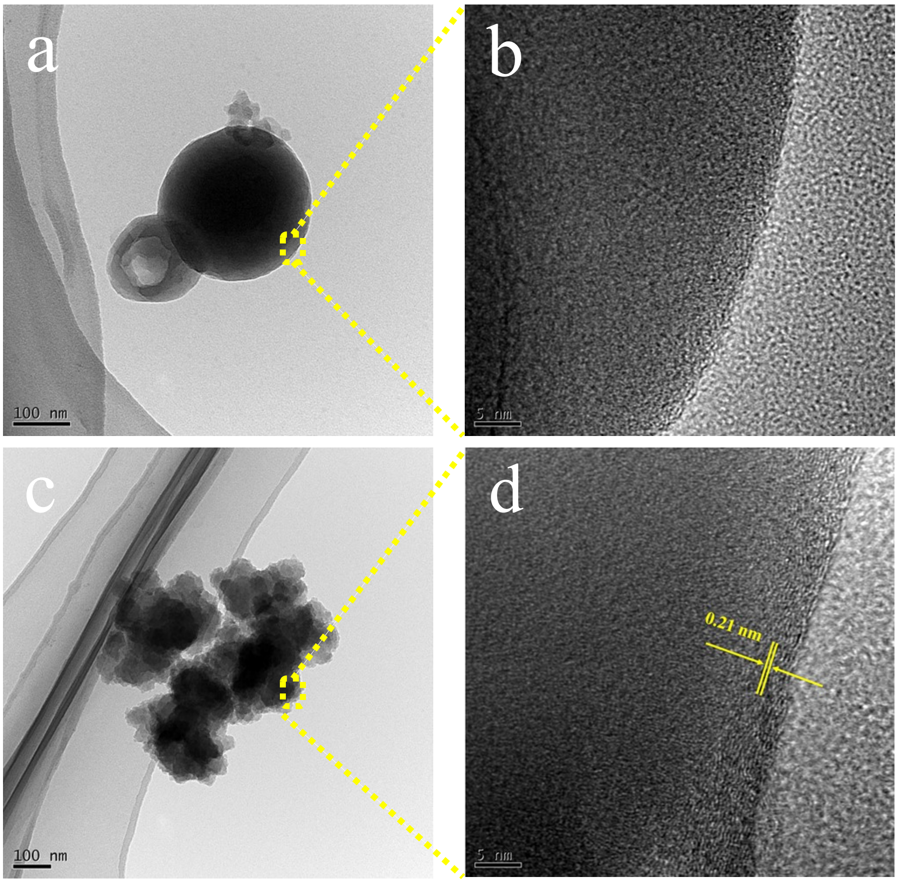

Fig. S4 HRTEM images of a-b) AlHCF and c-d) AlHCF/Gr.

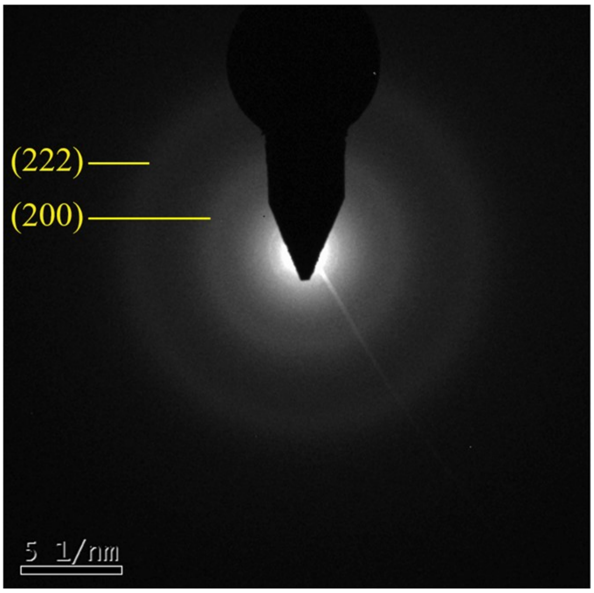

Fig. S5 The selected area electron diffraction (SAED) patterns of AlHCF. The diffraction ring of AlHCF confirms its po lycrystalline characteristics.

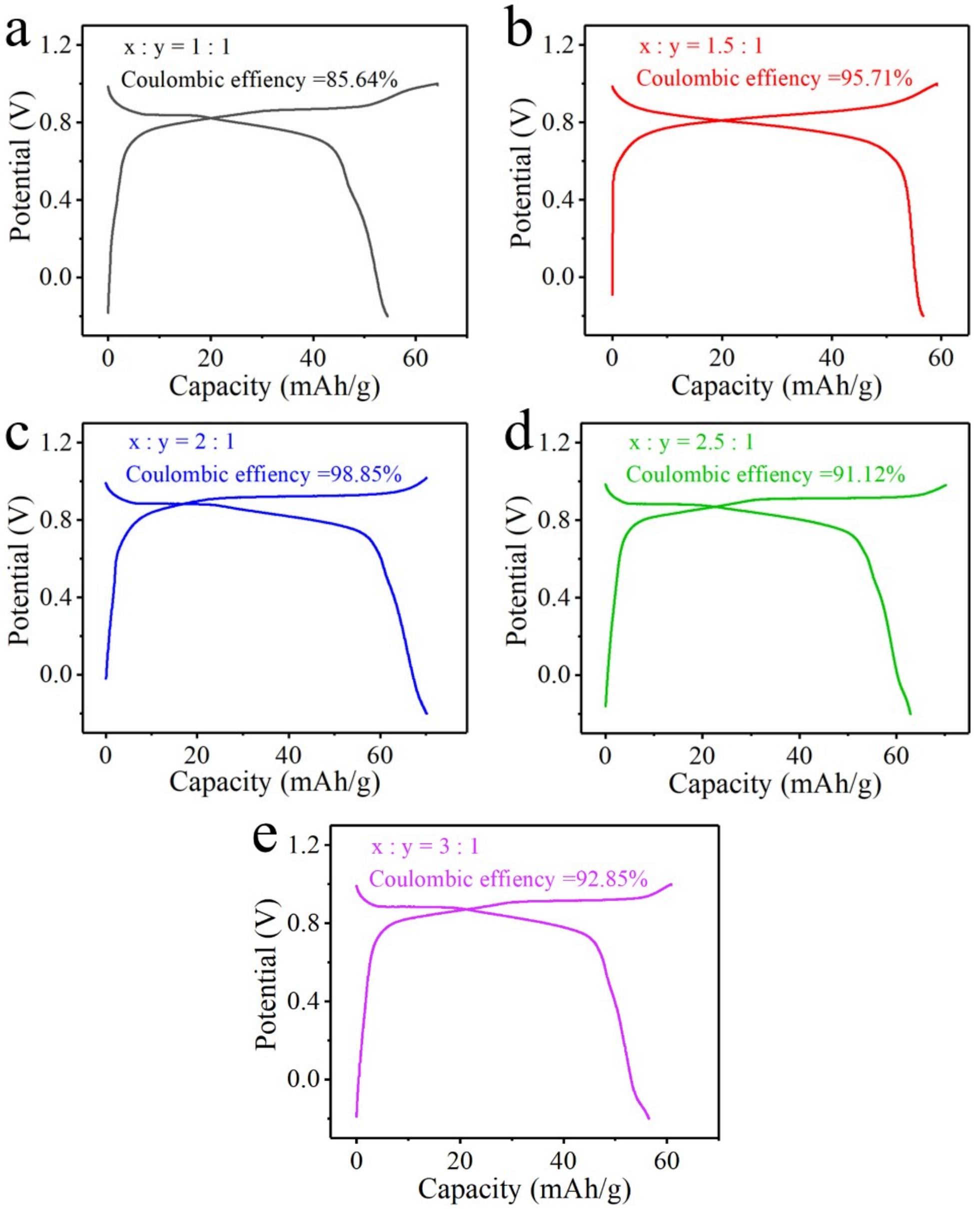

Fig. S6 a-e) Galvanostatic charge/discharge (GCD) profiles at maximum capacity for different ingredient proportion of AlHCF, x:y represents the ingredient proportion of Al^{3+} : $Fe(CN)_6^{4-}$.

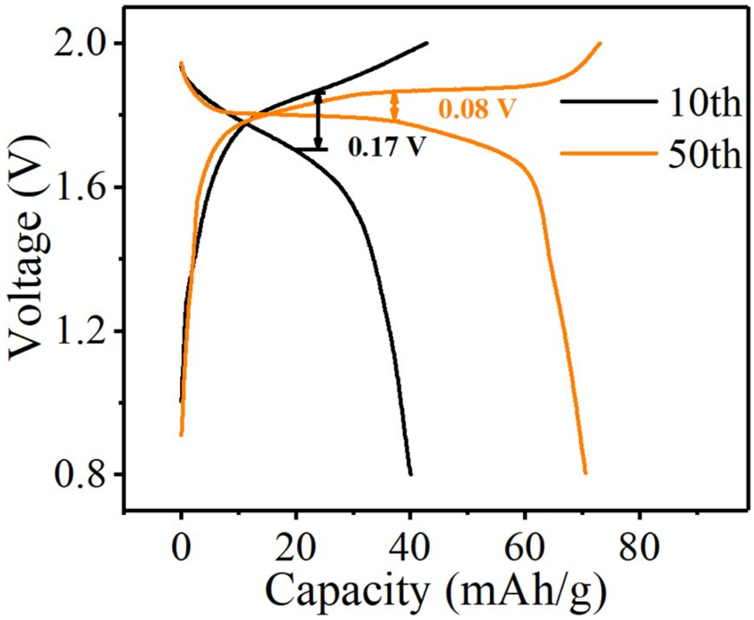

Fig. S7 Voltage difference between the charge and discharge plateaus of cycle 10 and cycle 50.

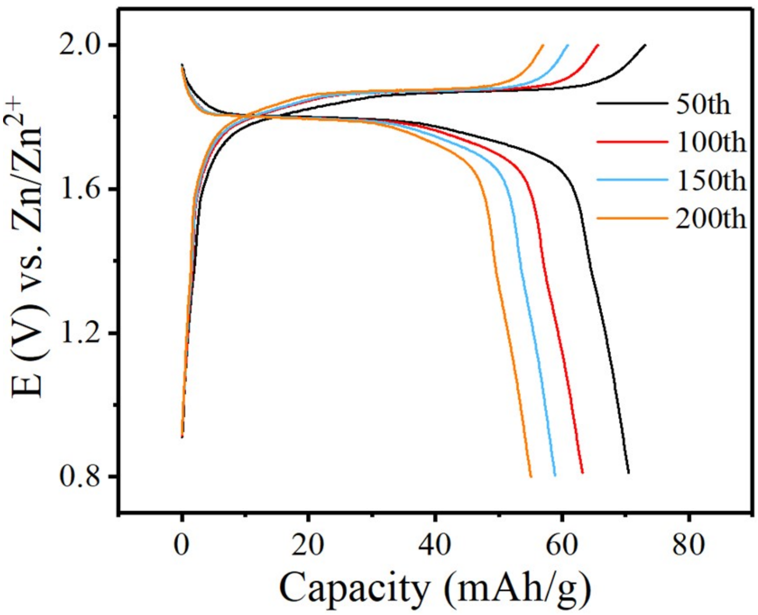

Fig. S8 GCD profiles of long-term cycle.

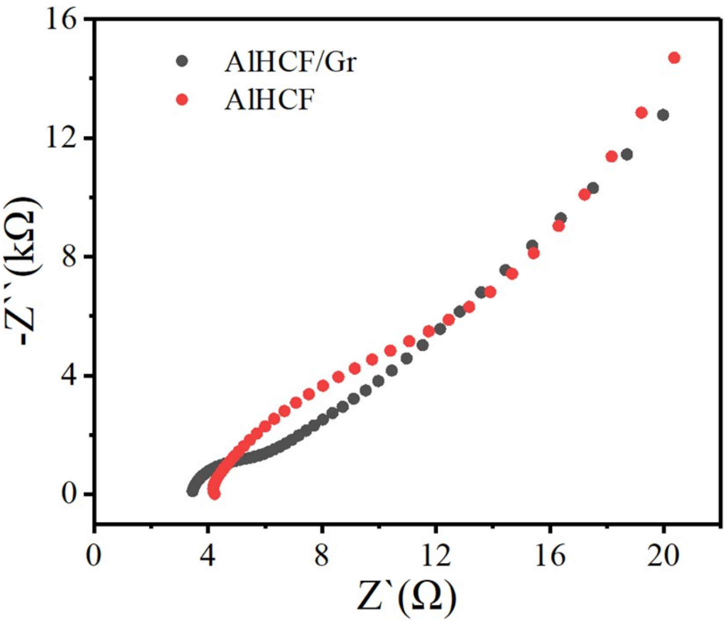

Fig. S9 Electrochemical impedance spectroscopy (EIS) of AlHCF and AlHCF/Gr.

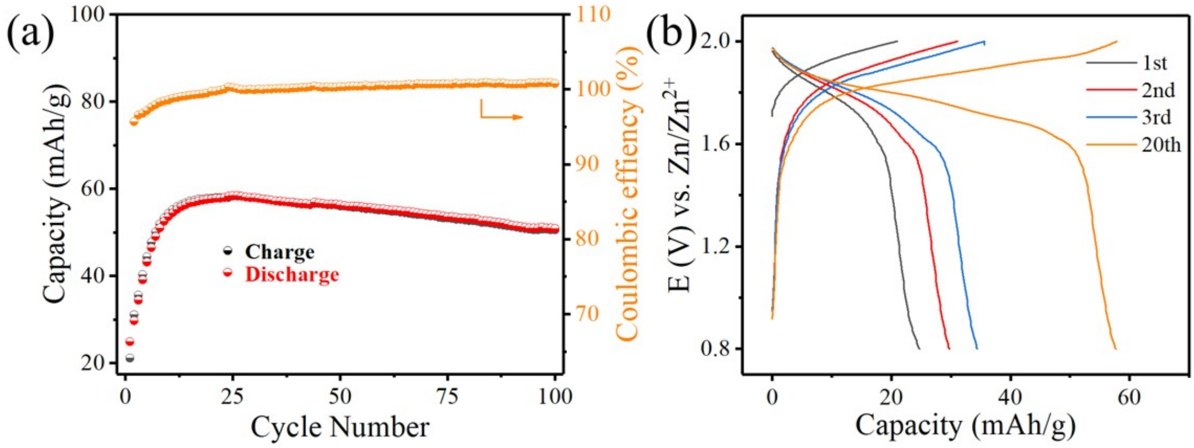

Fig. S10 Electrochemical performance of full cell at 5C (1C=60 mA g-1). a) Cycling performance of full cell using AlHCF/Gr as cathode. b) GCD profiles of full cell.

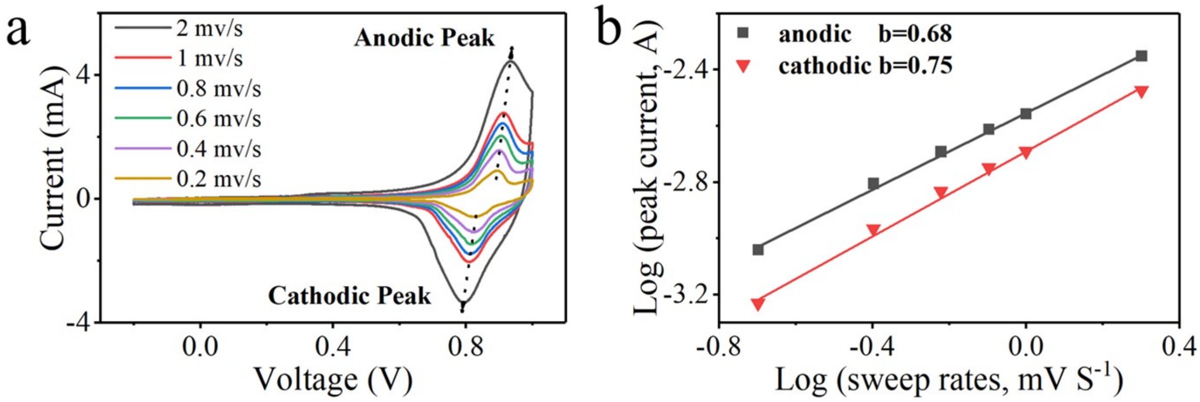

Fig. S11 Electrode kinetics analysis of AlHCF/Gr electrode with cycling. a) Cyclic voltammograms of AlHCF at various scan rates. b) log(i) - log(v) plots of anodic and cathodic peaks derived from the scan rate dependent CV curves.

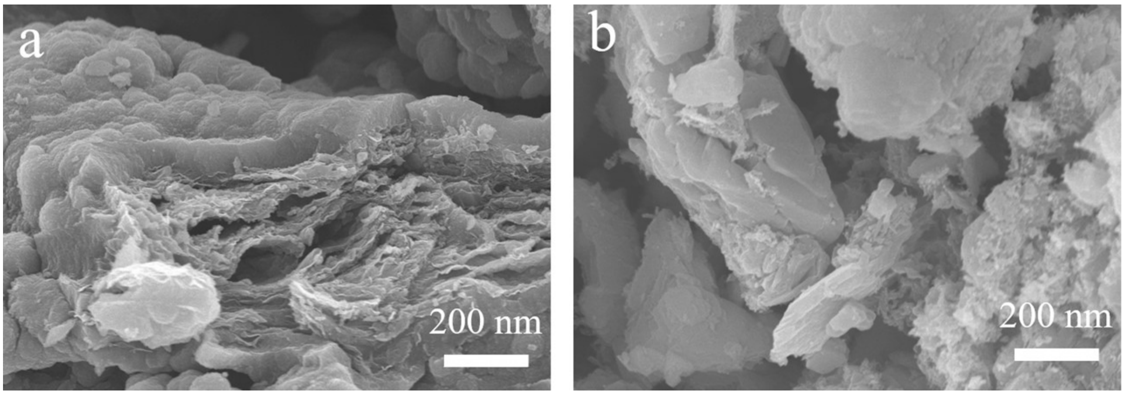

Fig. S12 SEM images of AlHCF/Gr a) before and b) after 200 cycles.

Table S1 Structural parameters of AlHCF after Rietveld refinement.

Space group	Fmm
a	9.97882 Å
b	9.97882 Å
c	9.97882 Å
α	90°
β	90°
γ	90°
Cell volume	993.65970 $Å^3$
R_{wp}	7.46%
R_p	5.54%

Table S2 Fractional coordinates of AlHCF after Rietveld refinement.

Atom	Wyckoff position	x	y	z	Occupancy
Al	4b	0.5000	0.0000	0.0000	1
Fe	4a	0.0000	0.0000	0.0000	1
C	24e	0.2033	0.0000	0.0000	1
N	24e	0.3086	0.0000	0.0000	1
K	8c	0.2500	0.2500	0.2500	0.0304

Table S3 Element content of AlHCF.

Unit: wt%

Sample	ICP-AES			EA		TGA
	K	Al	Fe	C	N	H_2O
AlHCF	1.41	13.79	10.18	24.27	23.41	23.0

Table S4 Comparison of energy densities & average operating voltage of zinc-ion batteries using different PBAs materials as cathode. Energy density is calculated based on the total mass of active electrode materials.

Anode/Cathode	Average operating voltage / V	Energy density / Wh kg^{-1}	Reference
Zn/ZnHCF	1.7	100	1
Zn/ZnHCF	1.73	104	2
Zn/KMnHCF	1.74	150	3
Zn/KNiHCF	1.19	67	4
Zn/NiHCF	1.2	60	5
Zn/KMnHCF	1.4	99	6
Zn/CuHCF	1.73	93	7
Zn/CuZnHCF	1.73	62	8
Zn/FeHCF	1.2	72	9
Zn/NaFeHCF	1.1	81	10
Zn/FeHCF	1.1	50	11
Zn/AlHCF	**1.8**	**125**	**This work**

Table S5 Ionization Potential, Electronegativity and Radius for some ions.[12]

Ion	I_A (eV)	X_A	Radius (Å)
Fe^{2+}	30.6	23.4	0.61
Ni^{2+}	35.2	26.7	0.69
Cu^{2+}	36.8	28.6	0.73
Zn^{2+}	39.7	28.8	0.74
Mn^{2+}	33.7	24.4	0.67
Co^{3+}	51.3	—	0.65
Al^{3+}	120.0	74.2	0.54

I_A: Ionization Potential, X_A: Electronegativity.

Table S6 Refinement data for various MeHCFs. ZnHCF is a rhombohedral structure (space group R-3c).

Sample	Bond	Bond distance (Å)	Reference
NiHCF (Fm-3m)	Ni-N	2.043	13
	Fe-C	1.761	
	C≡N	1.150	
ZnHCF (R-3c)	Zn-N1	1.998	14
	Zn-N2	1.971	
	Fe-C1	1.907	
	Fe-C2	1.907	
	C1≡N1	1.161	
	C2≡N2	1.154	
CuHCF (Fm-3m)	Cu-N	2.069	15
	Fe-C	1.866	
	C≡N	1.180	
MnHCF (Fm-3m)	Mn-N	2.183	16
	Fe-C	1.863	
	C≡N	1.140	
CoHCF (Fm-3m)	Co-N	1.976	17
	Fe-C	1.882	
	C≡N	1.180	
AlHCF	Al-N	1.909	This work

(Fm-3m)	Fe-C	2.029	
	C≡N	1.051	

Reference

1. L. Zhang, L. Chen, X. Zhou and Z. Liu, Towards High-Voltage Aqueous Metal-Ion Batteries Beyond 1.5 V: The Zinc/Zinc Hexacyanoferrate System, *Advanced Energy Materials*, 2015, **5**, 1400930.
2. L. Zhang, L. Chen, X. Zhou and Z. Liu, Morphology-Dependent Electrochemical Performance of Zinc Hexacyanoferrate Cathode for Zinc-Ion Battery, *Scientific Reports*, 2015, **5**, 18263.
3. D. Wenjun, Z. Li, Y. Ye, Z. Zhou, Y. Li, M. Zhang, X. Yuan, J. Hu, W. Zhao, Z. Huang, C. Li, H. Chen, J. Zheng and R. Li, Zn^{2+} Induced Phase Transformation of K2mnfe(Cn)6 Boosts Highly Stable Zinc‐Ion Storage, *Advanced Energy Materials*, 2021.
4. M. S. Chae, J. W. Heo, H. H. Kwak, H. Lee and S.-T. Hong, Organic Electrolyte-Based Rechargeable Zinc-Ion Batteries Using Potassium Nickel Hexacyanoferrate as a Cathode Material, *Journal of Power Sources*, 2017, **337**, 204-211.
5. A. L. Lipson, S.-D. Han, S. Kim, B. Pan, N. Sa, C. Liao, T. T. Fister, A. K. Burrell, J. T. Vaughey and B. J. Ingram, Nickel Hexacyanoferrate, a Versatile Intercalation Host for Divalent Ions from Nonaqueous Electrolytes, *Journal of Power Sources*, 2016, **325**, 646-652.
6. T. Cao, F. Zhang, M. J. Chen, T. Shao, Z. Li, Q. J. Xu, D. H. Cheng, H. M. Liu and Y. Y. Xia, Cubic Manganese Potassium Hexacyanoferrate Regulated by Controlling of the Water and Defects as a High-Capacity and Stable Cathode Material for Rechargeable Aqueous Zinc-Ion Batteries, *Acs Applied Materials & Interfaces*, 2021, **13**, 26924-26935.
7. R. Trócoli and F. La Mantia, An Aqueous Zinc-Ion Battery Based on Copper Hexacyanoferrate, *ChemSusChem*, 2015, **8**, 481-485.
8. G. Kasiri, J. Glenneberg, A. Bani Hashemi, R. Kun and F. La Mantia, Mixed Copper-Zinc Hexacyanoferrates as Cathode Materials for Aqueous Zinc-Ion Batteries, *Energy Storage Materials*, 2019, **19**, 360-369.
9. Z. Liu, G. Pulletikurthi and F. Endres, A Prussian Blue/Zinc Secondary Battery with a

Bio-Ionic Liquid–Water Mixture as Electrolyte, *ACS Applied Materials & Interfaces*, 2016, **8**, 12158-12164.

10. L.-P. Wang, P.-F. Wang, T.-S. Wang, Y.-X. Yin, Y.-G. Guo and C.-R. Wang, Prussian Blue Nanocubes as Cathode Materials for Aqueous Na-Zn Hybrid Batteries, *Journal of Power Sources*, 2017, **355**, 18-22.
11. Z. Liu, P. Bertram and F. Endres, Bio-Degradable Zinc-Ion Battery Based on a Prussian Blue Analogue Cathode and a Bio-Ionic Liquid-Based Electrolyte, *Journal of Solid State Electrochemistry*, 2017, **21**, 2021-2027.
12. R. G. Parr and R. G. Pearson, Absolute Hardness: Companion Parameter to Absolute Electronegativity, *Journal of the American Chemical Society*, 1983, **105**, 7512-7516.
13. G. Małecki and A. Ratuszna, Crystal Structure of Cyanometallates $Me_3[Co(CN)_6]_2$ and $Kme[Fe(CN)_6]$ with Me=Mn^{2+}, Ni^{2+}, Cu^{2+}, *Powder Diffraction*, 1999, **14**, 25-30.
14. J. Rodríguez-Hernández, E. Reguera, E. Lima, J. Balmaseda, R. Martínez-García and H. Yee-Madeira, An Atypical Coordination in Hexacyanometallates: Structure and Properties of Hexagonal Zinc Phases, *Journal of Physics and Chemistry of Solids*, 2007, **68**, 1630-1642.
15. R. Rigamonti, Struttura Dei Cupriferrocianuri.- Nota Ii. Ferrocianuri Di Rame E Cationi Monovalenti, *Gazzetta Chimica Italiana*, 1937, **67**, 146-158.
16. R. Martínez-García, E. Reguera, J. Rodriguez, J. Balmaseda and J. Roque, Crystal Structures of Some Manganese(Ii) and Cadmium Hexacyanoferrates (Ii,Iii) and Structural Transformations Related to the Sorption of Cesium, *Powder Diffraction*, 2004, **19**, 255-264.
17. R. Rigamonti, Struttura E Costituzione Chimica Di Alcuni Ferrocianuri, *Gazzetta Chimica Italiana*, 1938, **68**, 803-809.